A Novel DCT-Based Compression Scheme for 5G Vehicular Networks

Yuhan Su[®], Xiaozhen Lu[®], Lianfen Huang, Xiaojiang Du[®], *Senior Member, IEEE*, and Mohsen Guizani[®], *Fellow, IEEE*

Abstract—Next-generation (5G) vehicular networks will support various network applications, leading to specific requirements and challenges for wireless access technologies. This trend has motivated the development of the long-term evolution-vehicle (LTE-V) network, a 5G cellular-based vehicular technology. Due to the limited bandwidth for vehicular communications, it is important to efficiently utilize slim spectrum resources in vehicular networks. In this paper, we introduce a cloud radio access network (C-RAN)based vehicular network architecture, named C-VRAN, which facilitates efficient management and centralized processing of vehicular networks. Furthermore, we propose a discrete cosine transform (DCT)-based data compression scheme for C-VRAN to enhance the effective data rate of the fronthaul network. This scheme first uses DCT to perform time-frequency conversion of LTE-V I/Q data and then utilizes the Lloyd-Max algorithm to quantify data in the frequency domain before finally selecting an appropriate coding scheme to achieve better performance. Simulation results show that the proposed scheme can achieve 3 times compression ratio within 1% error vector amplitude distortion, and it also has strong independence and versatility, allowing it to be used as a standalone module for the current LTE-V system.

Index Terms—Data compression, vehicular networks, 5G, discrete cosine transform, Lloyd-Max.

I. INTRODUCTION

HE fifth-generation mobile communication system (5G) is a research hotspot in industry and academia [1], [2], with vehicular networks considered one of the most challenging 5G applications. Due to various time-sensitive applications, especially with automated driving and vehicular entertainment applications [3], vehicular networks must support stability, low latency, and secure communications along with high data transmission. Therefore, these networks require advanced wireless technologies to deploy 5G.

Manuscript received January 14, 2019; revised June 10, 2019 and August 5, 2019; accepted August 25, 2019. Date of publication September 5, 2019; date of current version November 12, 2019. This work was supported in part by the US National Science Foundation (NSF) under Grants CNS-1564128 and CNS-1824440. The review of this article was coordinated by Dr. A. J. Al-Dweik. (Corresponding author: Lianfen Huang.)

Y. Su, X. Lu, and L. Huang are with the Key Laboratory of Digital Fujian on IoT Communication, Architecture and Safety Technology, Xiamen University, Xiamen 361005, China (e-mail: suyuhan066@foxmail.com; 543luxiaozhen@gmail.com; lfhuang@xmu.edu.cn).

X. Du is with the Department of Computer and Information Sciences, Temple University, Philadelphia, PA 19122 USA (e-mail: dxj@ieee.org).

M. Guizani is with the Department of Computer Science and College of Engineering, Qatar University, 2713 Doha Al Tarfa, Qatar (e-mail: mguizani@ieee.org).

Digital Object Identifier 10.1109/TVT.2019.2939619

Various wireless access technologies can be used to provide the radio interfaces required for vehicular communications, such as Wi-Fi, IEEE 802.11p, and long-term evolution-vehicle (LTE-V) [4], [5]. These technologies generally offer diverse capabilities for vehicle communications; however, Wi-Fi cannot support high mobility over a small communication range. IEEE 802.11p faces notable shortcomings such as low reliability, hidden node problems, unrestricted delays, and intermittent vehicle-to-infrastructure (V2I) connections [6]–[8]. From an industrial perspective, the widespread deployment of IEEE 802.11p requires substantial investment in the network infrastructure.

This issue can be addressed by using long-term evolution (LTE) to support vehicular applications [9], [10]. LTE-V networks are widely used in the Chinese vehicular communications industry [11] and considered the best choice for effective intelligent transportation systems (ITS). Compared with other ITS solutions, LTE-V technology can make full use of base stations around the world to reduce deployment costs and time while providing comprehensive quality of service (QoS) support along with a high data rate, high penetration rate, and large coverage for V2I communications. However, how to effectively allocate resources to meet vehicular service requirements with limited resource range and large-scale network topology [12] is a key issue for LTE-V.

The cloud radio access network (C-RAN) [13] will be an important network architecture in future cellular networks; it is a green radio access network architecture based on centralized processing, collaborative radio and real-time cloud infrastructure, which can support cellular network systems and future wireless communication standards. By implementing a baseband unit (BBU) centralization at the C-RAN hub, a new physical layer called fronthaul is introduced into the network. Fronthaul is the link between the BBU pool and the remote radio unit in the macro-cell base stations or small-cell base stations site. Fibers can provide more bandwidth, so it is the best choice for the prequel. Accordingly, C-RAN appears a promising access architecture for LTE-V networks due to its processing ability and flexible management. Thus, in this paper, we develop a C-RAN based vehicular network architecture named C-VRAN. As shown in Fig. 1, the BBUs and LTE-V cells are physically separated, and baseband processed signals are transported between LTE-V cells and BBU through the fronthaul. This architecture can balance traffic between BBUs according to mobile network load shifts by breaking the static

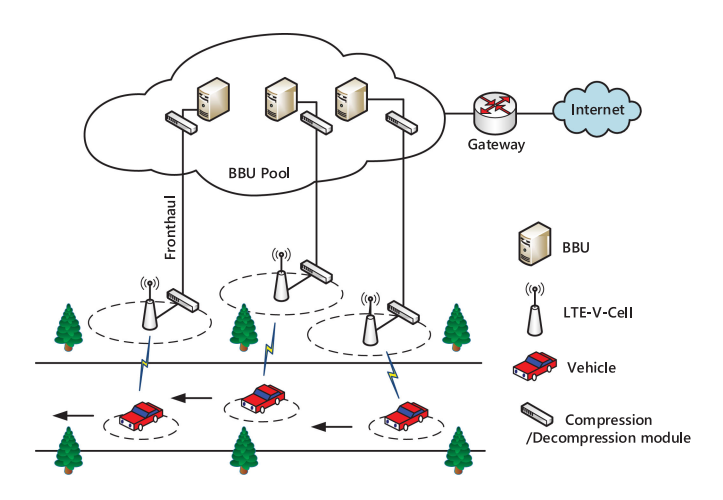


Fig. 1. Illustration of a C-RAN based vehicular networks architecture.

connection between LTE-V cells and BBUs, thus offering a great potential to increase data rates in a cost-effective manner. The fronthaul requires a high bandwidth as the throughput of the baseband radio signal is an order of magnitude higher than that of the carried IP payload. Several methods deploy more links connecting the BBUs and LTE-V cells to improve the fronthaul data rate, but such deployment would carry extraordinarily high costs. Therefore, we deploy the data compression module over fronthaul links to realize a tradeoff between the deployment cost and high fronthaul data rate. Fronthaul link compression can greatly reduce the required cost for the C-VRAN and upgrade the data rate and potentially realize a valuable change in the existing distributed base station or C-RAN architecture.

Motivated by the above observations from technical and industrial perspectives, we propose a data compression scheme to ensure a minimal change in C-VRAN architecture. The compression scheme uses the energy compaction characteristics of discrete cosine transform (DCT) to select and process frequency-domain coefficients. Data is divided into blocks of high-frequency components, quantized with fewer bits and lowfrequency components, and blocks quantized with more bits. The proposed scheme also involves the selection and use of common compression coding methods (e.g., Lloyd-Max quantization and Huffman coding) to make the scheme adaptively determine the best bit allocation and learn the optimal codebook. For instance, we can use the algorithm of row-column separation for the LTE baseband signal (i.e., I-component data and Q-component data undergo respective DCT) to use the onedimensional DCT fast operator and implement the algorithm directly and easily with a program or hardware structure. The main contributions of this paper are as follows.

- We present a novel C-RAN-based vehicular network architecture (C-VRAN), which is a centralized, cloudcomputing-based vehicular access network, to facilitate centralized processing, dynamic scheduling, and allocation of resources in vehicular networks.
- We propose a DCT-based data compression scheme for C-VRAN that divides data into two blocks in the frequency

domain, quantifies the data blocks, and adaptively selects an appropriate coding method. Simulation results reveal that this scheme effectively reduces the amount of data transmitted between the BBU and the LTE-V cell.

The rest of this paper is organized as follows. Section II reviews related work. Section III describes the DCT-based data compression scheme in detail, including signal analysis and a discussion of each submodule. Section IV presents the simulation results to validate the proposed scheme. Finally, Section V concludes the paper.

II. RELATED WORK

Research on vehicular network architecture has attracted extensive attention from industry experts, operators, and scholars. The authors in [14] proposed a 5G vehicular ad hoc network architecture based on software-defined network (SDN), where neighboring vehicles can cluster adaptively according to realtime road conditions using the global information collection and control functions in SDN. The authors in [15] put forth a new vehicular network architecture integrating 5G mobile communication technologies and SDN; additionally, fog cells were deployed at the edge of 5G software-defined vehicular networks, which utilized multihop relays to reduce frequent handover between the road side units and vehicles. A new 5G-enabled vehicular network paradigm was developed in [16], which extended the C-RAN to integrate local cloud services to provide a low-cost, scalable, self-organizing, and effective solution. In [17], the authors conducted a comprehensive survey of C-RAN and fog network structures and investigated possible harmonization to integrate the two and meet the diverse needs of 5G vehicular networks. The authors of [18] designed a new V2X architecture based on 5G network slicing, in which vehicles can configure logical network functions and parameters to customize the specific service requirements they need. Despite these novel models, mobility management and resource allocation problems in next-generation vehicular networks require further research.

Few data compression schemes exist for vehicular networks; however, relevant research has been conducted with cellular networks. In LTE systems, the sampling rate exceeds the signal bandwidth, which results in redundancy in the frequency domain; about one-third of the spectrum does not carry information relevant to LTE transmission. To solve this problem, [19] proposed a non-linear scalar quantization-based data compression scheme that uses a multi-rate filter to downsample data, removing redundancies and substantially reducing the transport data rate while maintaining low levels of signal distortion to realize a lower-cost transport network. The authors in [20] put forth a compression scheme exploiting the temporal and spectral features of baseband signals based on [19]; they then used the Lloyd-max quantizer to adaptively adjust the quantization interval using the statistical structure of the baseband signal to achieve a high compression ratio and low latency with limited effect on end-to-end communication. In [21], the author devised a data compression scheme based on automatic gain control

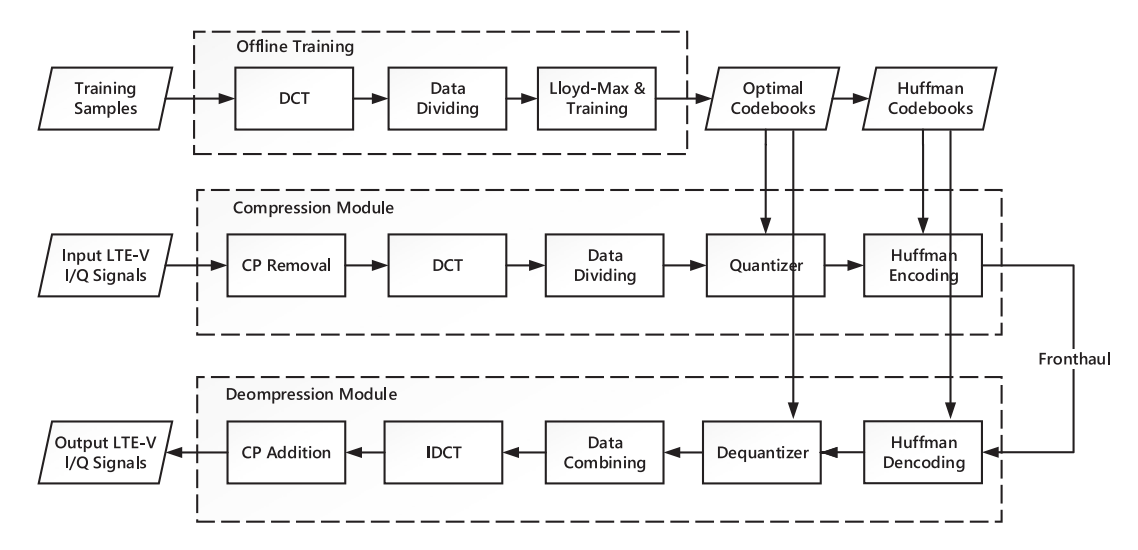


Fig. 2. Illustration of the DCT-based compression scheme Flowchart.

(AGC). This scheme applied a modified AGC algorithm with low latency and low complexity to scale data blocks, achieving an approximate 30% compression ratio with an EVM close to 2%. A compression scheme based on an improved fast K-means clustering algorithm was presented in [22]. This scheme considered vector quantization (VQ) instead of scalar quantization, taking advantage of the temporal correlation of I/Q data to minimize common public radio interface transmission bandwidth in the C-RAN under an assumed EVM of less than 0.025%; the data compression ratio reached approximately 4%, particularly in low-throughput conditions. In [23], the authors proposed a VQbased compression algorithm by vectorizing LTE I/Q samples and improving initialization of the Lloyd-Max algorithm for codebook offline training. Entropy coding was introduced in the final compression step, which further improved the compression gain.

Of the aforementioned related work, [19]–[21], [23], they used a multi-rate filter for data downsampling before data compression, which can be useful for data volume reduction. However, our proposed scheme optimizes data of the high-frequency component and the low-frequency component separately; and retains high-frequency information, thereby reducing loss of the original signal. On the other hand, the compression scheme mentioned in [20] also used Lloyd-Max quantization, which requires minimization of the mean square error for iterative calculation along with a large extent of calculation. Comparatively, our proposed scheme sets the quantizing module and encoding module outside the system (i.e., offline training) so the system calculation only requires time-frequency transform and coding and decoding according to the codebook; hence, the extent of calculation is small.

III. A DCT-BASED COMPRESSION SCHEME

A. System Flowchart

The system flow chart for the proposed DCT-based compression scheme is illustrated in Fig. 2. The whole system contains compression module, decompression module, offline training

module and transmission module. For downlink transmission, the compression module at the BBU pool site contains cyclic prefix (CP) removal module, DCT module, data dividing module, quantizing module, and Huffman encoding module. The decompression module at the LTE-V cell site contains Huffman decoding module, dequantizing module, data combining module, inverse DCT (IDCT) module, and CP addition module. The transmission module is the fronthaul link, which is used to transmit the data after compression. The input of the compression module is a stream of digital I/Q samples generated by the physical layer of LTE-V system. In addition, we set up an offline training module outside the system to train the optimally quantized codebook. Next, we introduce the functions of these modules in detail.

B. Cyclic Prefix Removal

To avoid inter-symbol interference in multipath fading channels, each symbol has a CP at its own head, which is copied from the end of the symbol [24]. The CP creates a guard period before the inverse fast Fourier transform (IFFT) output. However, in terms of compression, CP represents a source of time-domain redundancy, which the CP removal module in the compression module is intended to eliminate. The compression gain CR_{cp} from this module can be expressed as

$$CR_{cp} = \frac{L_{sym} + L_{cp}}{L_{sym}},\tag{1}$$

where L_{sym} denotes the IFFT output symbol length, and L_{cp} denotes the CP length, respectively.

C. Time-Frequency Transform and Signal Analysis

The DCT represents a finite sequence of data points based on the sum of cosine functions oscillating at different frequencies, which is a Fourier-dependent transform similar to discrete Fourier transform (DFT) but using only real numbers. DCT is important for many applications in science and engineering, from lossy compression of audio and images to spectral

methods for numerical solutions of partial differential equations. Two-dimensional DCT is commonly used for signal and image processing, especially for lossy compression, because it has a strong "energy compaction" property; that is, most signal information tends to be concentrated in a few low-frequency components of the DCT. Therefore, in the transform matrix orthogonal transform of speech and image signal transformation, the DCT is considered a quasi-optimal transform. In a series of international standards for video compression coding released in recent years, DCT is regarded as a basic processing module.

We select DCT for time-frequency transform due to its "energy compaction" property. The original signals and the training samples are passed through the following mathematical transformation before the data division:

$$F(k) = \sqrt{\frac{2}{N}} \sum_{n=0}^{N-1} c(k) f(n) \cos \frac{(2n+1)k\pi}{2N}, \qquad (2)$$

where N is the length of input signals, f(n) represents the main input data, F(.) represents the array of DCT coefficients and $k=0,1,\ldots,M-1$. The coefficient c(k) can be defined as:

$$c(k) = \begin{cases} \frac{1}{\sqrt{2}}, & k = 0; \\ 1, & k \neq 0. \end{cases}$$
 (3)

We observe data generated by an LTE-V link-level simulation platform and find that after the DCT of the derived data, signal information is distributed from the low-frequency domain to the high-frequency domain. Most signal information is concentrated in the low-frequency domain with a small part in the high-frequency domain, as shown in Fig. 3. Fig. 3(a) depicts the time-domain LTE-V I-component signals of a 10 MHz bandwidth 16 QAM system bandwidth of a physical sidelink shared channel (PSSCH); the data length is a radio frame (15.36 MHz \times 10 ms = 153600).

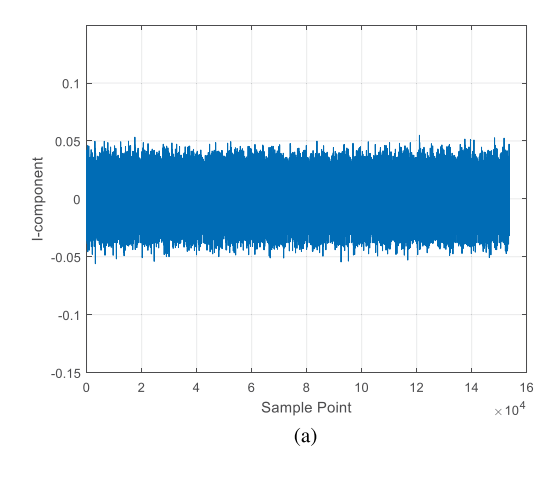
Using this feature, we can divide the frequency domain data into a low-frequency component block (Data Block 1) and high-frequency component block (Data Block 2) according to the energy distribution (see Fig. 3(c)), which is beneficial for efficient data compression and quantization coding.

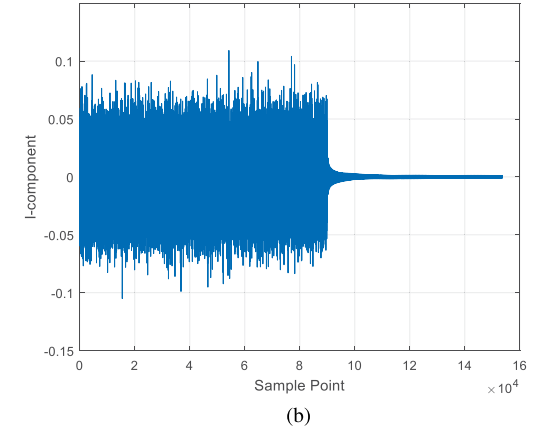
D. Codebook Training and Quantizing

After dividing the data into two blocks, the data samples are input into the training module. Considering the calculation delay of the system, we set the training module outside the system (i.e., offline training).

The first step in training is quantification. For a given quantization step size, in order to reduce the mean square error (MSE), we should reduce the step size when the probability density function is large, and increase the step size when it is small. So our quantizer codebook is trained using the Lloyd-Max algorithm [25], [26].

The Lloyd-Max quantizer is a non-uniform quantizer that minimizes the average distortion. For a given quantization step size, the quantization codebook can be uniquely determined by the source distribution. For continuous analog signals, the





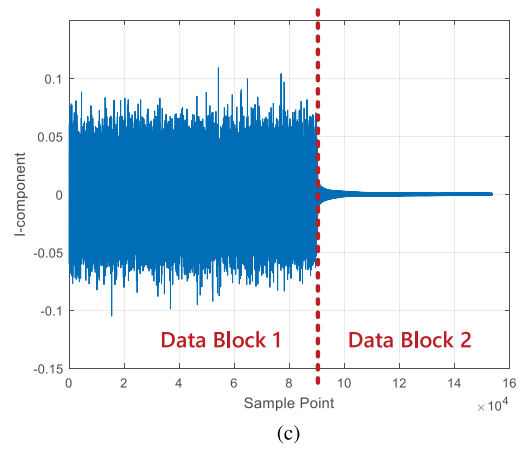


Fig. 3. Signal analysis of LTE-V PSSCH reference I-component signals with 16 QAM and 10 MHz bandwidth. (a) Time-domain signal. (b) Frequency-domain signal after DCT. (c) Illustration of data dividing.

algorithm uses a probability distribution function as input to identify the best quantized regions and values.

For the input signal distribution functions p(x), the quantitative output is $\widetilde{x_k}$. The number of quantization levels is M; the quantization interval endpoint value is denoted by x_k . When $x_{k-1} < x < x_k, x_k$ quantify to $\widetilde{x_k}$, then the MSE is:

$$D = \sum_{k=1}^{M} \int_{x_{k-1}}^{x_k} (x - \widetilde{x_k})^2 p(x) dx.$$
 (4)

To minimize the MSE, we take the derivative of $\widetilde{x_k}$ and x_k simultaneously. Then, we have:

$$x_k = \frac{1}{2}(\widetilde{x_{k+1}} + \widetilde{x_k}), \quad k = 1, 2, \dots, M - 1,$$
 (5)

$$\widetilde{x_k} = \frac{\int_{x_{k-1}}^{x_k} x p(x) dx}{\int_{x_{k-1}}^{x_k} p(x) dx}, \quad k = 1, 2, \dots, M.$$
 (6)

Continuous iteratives for (5) and (6) are calculated to minimize D, after which x_k and $\widetilde{x_k}$ are updated. The Lloyd-Max algorithm has been widely used in the communication field, such as solving channel estimation [27], [28], channel quantization [29] problems and reducing computational complexity of the system [30], [31].

For discrete digital signals, the input to the Lloyd-Max algorithm is the training sequence [32]. First, the initial quantization regions is set for the received samples according to the quantization level, then the optimal representation points for each region is calculated, and then the boundaris and the representation points are updated by iteration to minimize the total error between the representation points and the received samples.

Because the two data blocks have different probability mass distributions, we use the Lloyd-Max quantizer to optimize the optimal quantization of Data Blocks 1 and 2, respectively. We define the total quantization step size as Q:

$$Q = a + b, (7)$$

where $a \in \{1,2,\ldots,Q-1\}$ is the quantization step size of Data Block 1, and b=Q-a is the quantization step size of Data Block 2. To obtain the optimal quantization step size allocation for the two data blocks, we use the utility denoted by u to represent the gain of quantization step size distribution per unit of compression gain:

$$u(a,b) = \frac{EVM}{CR_q},\tag{8}$$

where EVM is the error vector magnitude of current a, CR_q is the current quantization gain.

$$CR_q = \frac{L_{sym} \cdot Q_0}{L_a \cdot a + L_b \cdot b},\tag{9}$$

where L_{sym} is the input data length, and L_a and L_a are the respective data lengths of Data Blocks 1 and 2. Q_0 is the uncompressed bitwidth of the I/Q component of input data. Therefore, our training problem is to minimize u(a,b) given by Q. The framework of the offline training module is illustrated in Fig. 4. As the input of the offline learning module, the value of Q maps the compression ratio; a smaller value achieves a high compression ratio and vice versa.

Due to the small number of training states, we can traverse all distribution possibilities of allocation of the quantization step size when Q is definite. Fig. 5 presents the allocation of the quantization step size for LTE-V data with 16 QAM and 10 MHz bandwidth when Q=12; in this case, u obtains the minimum value when a=9; the optimal allocation of the quantization step size is a=9, b=2.

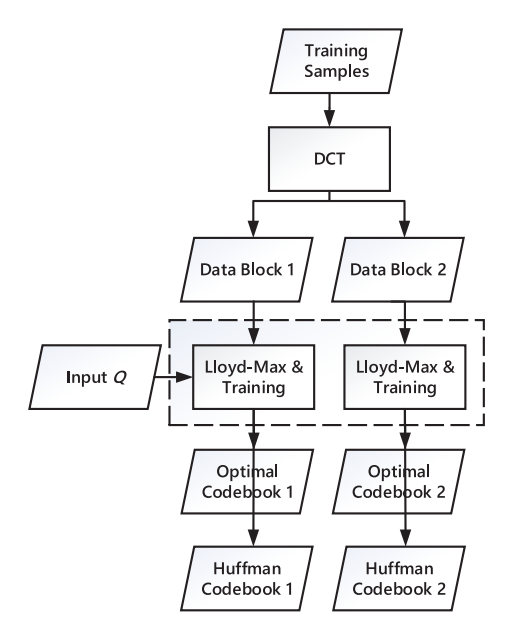


Fig. 4. Illustration of offline training module framework.

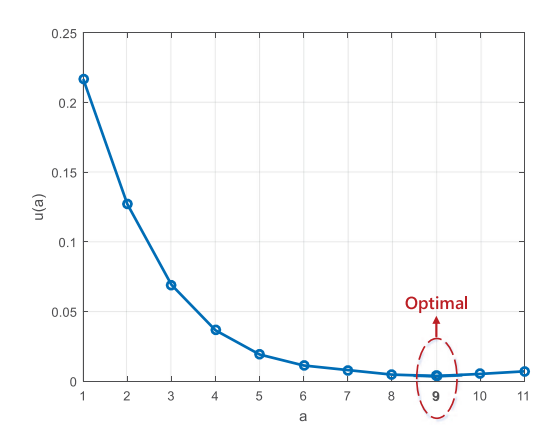


Fig. 5. Distribution possibilities of u of quantization step size for LTE-V data with 16 QAM and 10 MHz bandwidth when Q=12.

After the two-stage optimization (quantification and training), the training module will output the codebooks corresponding to the two data blocks under the optimal allocation bit. The output codebook can be further optimized via Huffman coding. The system will store the optimal codebooks after training in the system. We simulated the experiment multiple times once the system parameters were determined. The probability mass distribution of each data block was not substantially different. Therefore, the optimal codebook can be directly called for quantization and coding, and no retraining is needed, which reduces the computational complexity of the system.

E. Huffman Coding

According to the theory of communication [33], the theoretical limit of data compression is the information entropy of the data, after which the optimal data compression coding method can be determined. If the amount of information is not required to

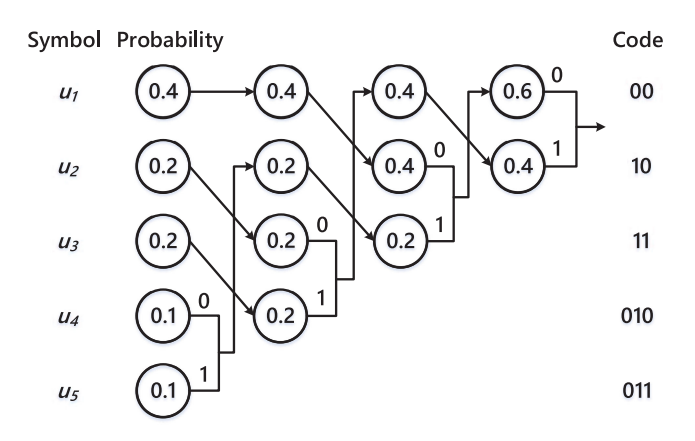


Fig. 6. Illustration of Huffman coding in this paper.

be lost in the encoding process, then information entropy must be preserved. This information is encoded as entropy coding based on the probability distribution characteristics of message occurrence, thus allowing for lossless data compression coding.

Huffman coding [34] is a common entropy coding scheme involving variable-length coding. The scheme constructs a codeword with the shortest average length of the heterogram head according to the likelihood of character occurrence. The Huffman code is optimal with linear time complexity for symbol-by-symbol coding [35], hence being otherwise known as "optimal encoding". The simplest Huffman coding construction algorithm uses a priority queue, in which the lowest-probability node is assigned the highest priority.

In this paper, we assume that data were quantized by the optimal codebook to generate five symbols u_1, u_2, u_3, u_4 and u_5 with corresponding respective probabilities of $P_1 = 0.4, P_2 = 0.1, P_3 = P_4 = 0.2$ and $P_5 = 0.1$. First, the symbols are arranged by probability from largest to smallest as indicated in Fig. 6. When encoding, starting with two symbols of minimum probability, one branch can be selected as 0 while the other is 1. Here, we deemed the upper branch 0 and the lower branch 1. The probabilities of the encoded branches are then combined and re-queued. The above steps can be repeated until the merge probability is normalized.

We can see that each codeword of the quantization codebook needs $L_a \cdot a + L_b \cdot b$ bits for representation without Huffman coding. However, we observe that the probability mass function of the codewords of the two data blocks is not uniform by multiple statistics, which means that there is a potential entropy coding gain. We assume that the average length of the Huffman code is expressed as Lhuff, then the compression gain of the Huffman coding is

$$CR_{huff} = \frac{L_a \cdot a + L_b \cdot b}{L_{huff}}. (10)$$

We can add the Huffman coding into the iteration of quantizing to optimize the codeword length.

TABLE I SIMULATION CONFIGURATION IN DIFFERENT CASES

Case Index	Bandwitch	Modulation Scheme
1	10 MHz	QPSK
2	20 MHz	QPSK
3	10 MHz	16QAM
4	20 MHz	16QAM
5	10 MHz	64QAM
6	20 MHz	64QAM

IV. SIMULATION AND NUMERICAL RESULTS

A. Simulation Scenario and Parameter Configurations

The LTE-V system is defined on the basis of LTE and LTEdevice-to-device (D2D). The physical layer of LTE-V follows some features of LTE and LTE-D2D, but also some changes have been made to the application scenario of V2X. According to 3GPP Release 14, LTE-V utilizes single carrier frequency division multiple access, supports QPSK and 16 QAM modulation technologies. Like the LTE system, LTE-V also supports 10 MHz and 20 MHz channels, each channel is divided into subframes, resource blocks (RBs) and subchannels. The subframe length is 1 ms, which is the same as the transmission time interval. The RB contains 12 subcarriers, each of which is 15 kHz bandwidth, so the total bandwidth of a RB is 180 kHz. LTE-V defines a subchannel as a group of RBs in the same subframe, and the number of RBs per subchannel can change with time. Subchannels are used to transmit data and control information. Data is transmitted over the PSSCH.

The 3rd Generation Partnership Project (3GPP) has begun to develop new 5G V2X enhancements under Release 15 and has completed an analysis of new use cases and requirements supported by this release [36]. As 64 QAM increases data rates and can reduce channel occupancy, 3GPP has identified the need for a new transmission of a demodulation reference signals scheme when introducing 64 QAM.

We present the LTE-V link level simulation according to the latest standard and generated the PSSCH reference signal to evaluate the performance of the proposed scheme. Different LTE-V link scenarios based on generated signals and detailed parameters of testing scenarios are listed in Table I. We set the data length of the training sample and the length of input signals to a radio frame; hence, the data compression cycle is a radio frame.

The error performance of the proposed scheme is quantified according to the EVM. The EVM indicates how closely the transmitter-generated I/Q component demodulates the signal to the ideal signal component, serving as an indicator of modulated signal quality. The EVM in this paper is defined as the ratio of the root mean square value of the average power of the error vector signal to the root mean square value of the average power of the ideal signal, expressed as a percentage. The smaller the

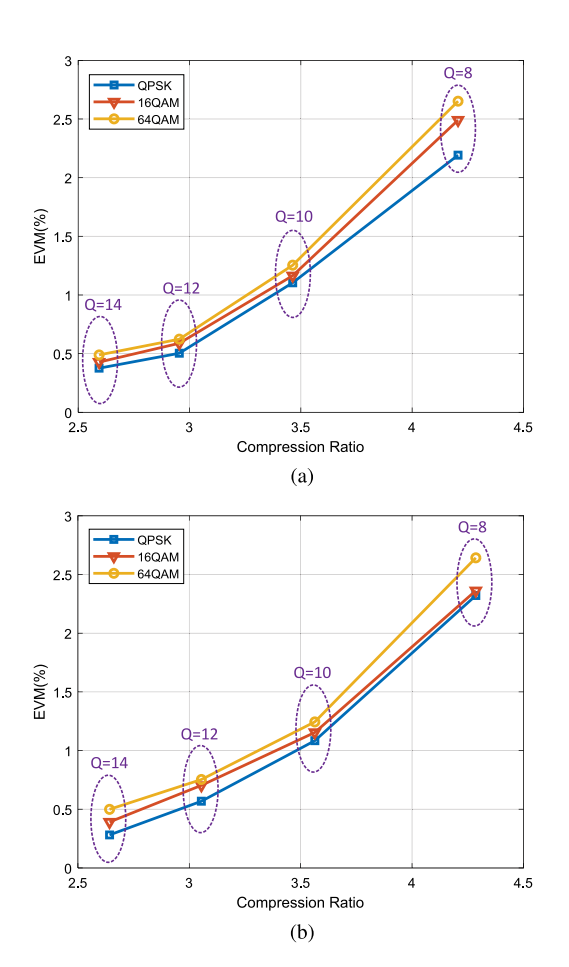


Fig. 7. Performance comparisons of EVM versus compression ratio with different modulation scheme and bandwidth. (a) 10 MHz. (b) 20 MHz.

EVM, the better the signal quality:

$$EVM = \sqrt{\frac{E[|\overline{f(n)} - f(n)|^2]}{E[|\overline{f(n)}|^2]}} \times 100\%,$$
 (11)

where f(n) is the original baseband signal before compression, and $\overline{f(n)}$ is the reconstructed baseband signal after compression and decompression.

Compression ratio in this work is defined as the ratio between the number of bits input into the data compression module and number of bits transmitted on fronthaul link. Because we finally transmit the Huffman-encoded codeword, the compression ratio can be expressed as

$$Compression\ ratio = \frac{(L_{sym} + L_{cp})Q_0}{L_{huff}}.$$
 (12)

Simulation results for 10 MHz and 20 MHz bandwidth are illustrated in Fig. 7. We simulate the EVM curve for Q=8,10,12,14. The results reveal that under the 2 times compression ratio, the EVM is within 0.5% or less in each case. The 2 times compression ratio indicates that if the original data were transmitted on two optical fibers in practical applications, the data can now be transmitted on only one optical fiber.

Table II presents the LTE downlink maximum EVM requirements for different modulation schemes according to the LTE

TABLE II LTE EVM REQUIREMENTS

Modulation Scheme	Maximum EVM(%)
QPSK	17.5
16QAM	12.5
64QAM	8

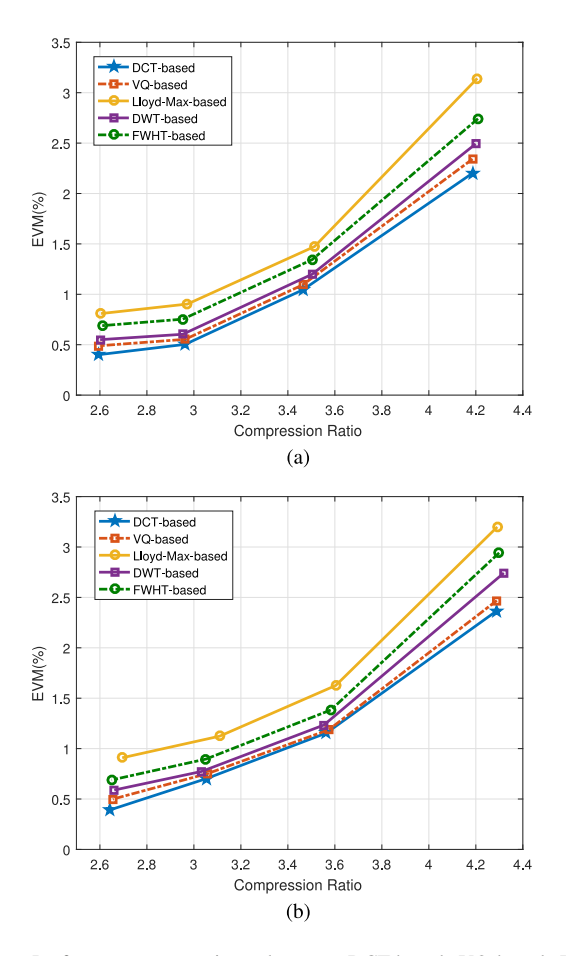
3GPP specification. We can see that the proposed scheme can achieve a compression ratio of 4 times with less than 2.5% EVM in high and low bandwidth scenarios, fully in line with engineering constraints.

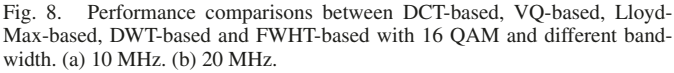
To compare the performance of our proposed scheme (DCT-based) and others, we arranged the following comparison schemes:

- 1) *VQ-Based:* A vector-quantization-based compression scheme was the adopted scheme in previous work [23].
- Lloyd-Max-Based: A compression scheme based on Lloyd-Max quantization removes the DCT module and data-dividing module from our proposed scheme.
- 3) DWT-Based: This compression scheme replaces the DCT module with the discrete wavelet transform (DWT) module in our proposed scheme. We used Haar wavelet as the wavelet basis function because it is orthogonal and simple. In this scheme, we quantized and encoded high-frequency wavelet coefficients and low-frequency wavelet coefficients after wavelet transform (the same as in our proposed scheme).
- 4) FWHT-Based: This compression scheme replaces the DCT module with the fast walsh hadamard transformation (FWHT) module in our proposed scheme. In this scheme, we divided, quantized, and encoded data according to the energy distribution of frequency domain coefficients following FWHT (the same as in our proposed scheme).

Fig. 8 shows that under the same bandwidth and modulation scheme, the proposed scheme performs best. This is mainly because the "energy compaction" property of DWT and FWHT was not as good as DCT for LTE-V data. Moreover, through experimental observation, the LTE-V baseband data exhibited irregular coefficient distribution in the frequency domain after FWHT, which is not conducive to subsequent data division and quantization.

To investigate the robustness of the proposed scheme and other compression techniques in terms of vehicle mobility, we used training samples generated by the 3GPP PSSCH reference channel with 16QAM modulation and 10 MHz bandwidth to train the codebook. The resultant codebook was then used to quantize sets of corresponding signals generated by the same channel model (i.e., the same modulation scheme and bandwidth), where the SNR changed from 0 dB to 30 dB under vehicle speed variations. The block error rate (BLER) versus SNR under vehicle mobility is illustrated in Fig. 9. Regarding compression from the proposed compression scheme and others, the BLER with 2 times compression ratio and without compression were





virtually indistinguishable. Yet at an approximate 4 times compression ratio, the proposed algorithm was the most robust. The DCT-based compression scheme was therefore robust against changes in channel conditions.

In addition, we compared the computational complexity of the proposed scheme and others. Because the processes of data dividing and Huffman encoding were the same, and the codebook training module was completed outside the system, we only needed to compare the computational complexity of the time-frequency transform for these schemes. The obtained results are listed as follows:

- 1) DCT-based: $O(N^2)$.
- 2) DWT-based: O(N).
- 3) FWHT-based: O(Nlog(N)).

Note that if we were to use the fast DCT algorithm for the time-frequency transform, the computational complexity of DCT would be O(Nlog(N)). Although the DWT-based scheme has less complexity than other compression schemes, the selection of different wavelet basis functions greatly influences the compression performance. The LTE adopts adaptive modulation and coding technology, wherein the network selects the best modulation and coding mode according to users' instantaneous channel conditions. If DWT is used to

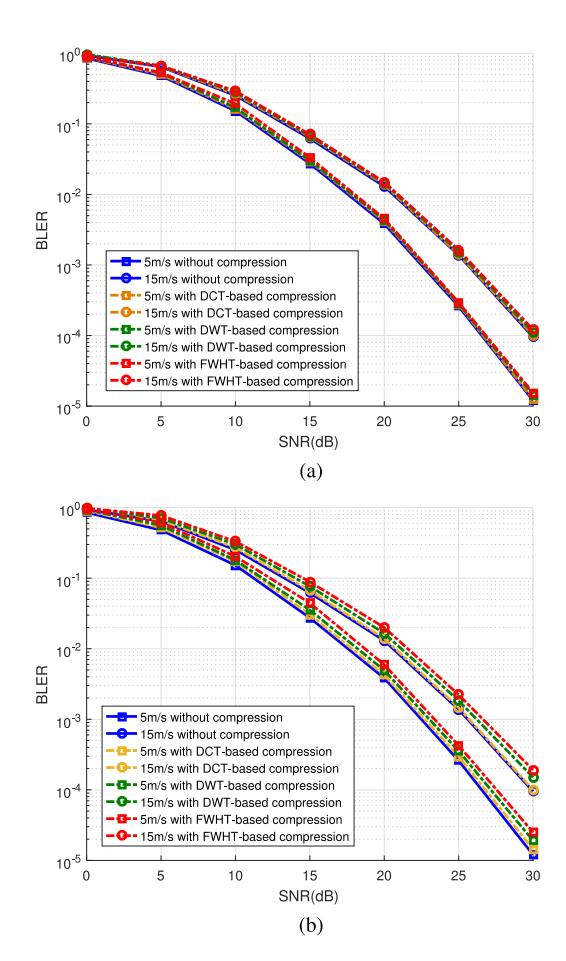


Fig. 9. BLER curves of simulation with and without implementation of compression. (a) Two times compression ratio. (b) Four times compression ratio.

perform the time-frequency transform on signals, then choosing the most suitable wavelet basis function according to different waveforms becomes complicated. Comparatively, DCT has a unique transformation basis function independent of signals, which facilitates engineering implementation. In addition, most industrial computers possess the calculation ability to support the computational complexity of the DCT-based scheme.

V. CONCLUSION

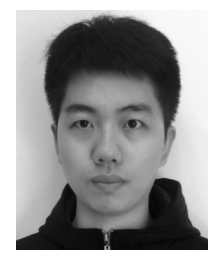
In this paper, we have proposed a C-RAN-based vehicular network architecture that can support the LTE-V network system for centralized processing, collaborative radio, and cloud computing. In addition, we have formulated a DCT-based compression scheme for the proposed architecture to provide compression gain by exploiting the frequency-domain characteristics of LTE-V I/Q samples. LTE-V Link-level simulation results have shown that the proposed scheme can achieve 2 times and 4 times compression ratio with approximate 0.4% EVM and 2% EVM distortion, respectively, which each out-perform previously reported performance. The simulation results have also demonstrated remarkable robustness of the proposed scheme in terms of vehicular mobility. Because our proposed scheme sets the codebook's construction module outside the system, it is better to train the sample to reflect the probability density

distribution of the data as much as possible to ensure decoding accuracy; a small amount will affect compression performance. In the future, we will improve the data compression scheme practically and implement the proposed scheme in multi-antenna scenarios. Note that the Lloyd-Max quantizer is a scalar quantizer, and the vector quantizer may perform better. Therefore, using vector quantizers for data quantification can also be an interesting future work.

REFERENCES

- METIS, "Mobile and wireless communications enablers for the 2020 information society," 2013. [Online]. Available: www.metis2020.com
- [2] T. O. Olwal, K. Djouani, and A. M. Kurien, "A survey of resource management toward 5G radio access networks," *IEEE Commun. Surv. Tut.*, vol. 18, no. 3, pp. 1656–1686, Third Quarter, 2016.
- [3] S. Y. Pyun, W. Lee, and D. H. Cho, "Resource allocation for vehicle-to-Infrastructure communication using directional transmission," *IEEE Trans. Intell. Transp. Syst.*, vol. 17, no. 4, pp. 1183–1188, Apr. 2016.
- [4] P. Papadimitratos, A. D. L. Fortelle, K. Evenssen, R. Brignolo, and S. Cosenza, "Vehicular communication systems: Enabling technologies, applications, and future outlook on intelligent transportation," *IEEE Com-mun. Mag.*, vol. 47, no. 11, pp. 84–95, Nov. 2009.
- [5] S. Al-Sultan, M. M. Al-Doori, A. H. Al-Bayatti, and H. Zedan, "A comprehensive survey on vehicular ad hoc network," *J. Netw. Comput.* Appl., vol. 37, pp. 380–392, Jan. 2014.
- [6] M. Amadeo, C. Campolo, and A. Molinaro, "Enhancing IEEE 802.11p/wave to provide infotainment applications in VANETs," Ad Hoc Netw., vol. 10, no. 2, pp. 253–269, Mar. 2012.
- [7] X. Du, Y. Xiao, S. Ci, M. Guizani, and H.-H. Chen, "A routing-driven key management scheme for heterogeneous sensor networks," *Proc. IEEE Int. Conf. Commun.*, 2007, pp. 3407–3412.
- [8] H. Hartenstein and K. Laberteaux, "VANET: Vehicular applications and inter-networking technologies," presented at the 1st ETSI Workshop ITS, 2010, pp. 1–17.
- [9] H. Zhang, S. Chen, X. Li, H. Ji, and X. Du, "Interference management for heterogeneous networks with spectral efficiency improvement," *IEEE Wireless Commun.*, vol. 22, no. 2, pp. 101–107, Apr. 2015.
- [10] S. Kato, M. Hiltunen, K. Joshi, and R. Schlichting, "Enabling vehicular safety applications over lte networks," in *Proc. Int. Conf. Connected Veh. Expo.*, Las Vegas, NV, USA, Dec. 2013, pp. 747–752.
- [11] S. C. *et al.*, "Vehicle-to-Everything (V2X) services supported by Ite-based systems and 5G," *IEEE Commun. Standards Mag.*, vol. 1, no. 2, pp. 70–76, Jun. 2017
- [12] X. Du, M. Zhang, K. E. Nygard, S. Guizani, and H.-H. Chen, "Self-healing sensor networks with distributed decision making," *Int. J. Sensor Netw.*, vol. 2, pp. 289–298, 2007.
- [13] "C-RAN the road towards green RAN," in China Mobile Research Institute, White Paper, v.3.0, 2013.
- [14] X. Duan, Y. Liu, and X. Wang, "SDN enabled 5G-VANET: Adaptive vehicle clustering and beamformed transmission for aggregated traffic," *IEEE Commun. Mag.*, vol. 55, no. 7, pp. 120–127, Jul. 2017.
- [15] X. Ge, Z. Li, and S. Li, "5G software defined vehicular networks," *IEEE Commun. Mag.*, vol. 55, no. 7, pp. 87–93, Jul. 2017.
- [16] R. Y. et al., "Optimal resource sharing in 5G-Enabled vehicular networks: A matrix game approach," *IEEE Trans. Veh. Technol.*, vol. 66, no. 10, pp. 7844–56, Oct. 2016.
- [17] S.-C. Hung, H. Hsu, S.-Y. Lien, and K.-C. Chen, "Architecture harmonization between cloud radio access networks and fog networks," *IEEE Access*, vol. 3, pp. 3019–3034, 2015.
- [18] C. Campolo, A. Molinaro, A. Iera, and F. Menichella, "5G network slicing for vehicle-to-Everything services," *IEEE Wireless Commun.*, vol. 24, no. 6, pp. 38–45, Dec. 2017.
- [19] D. Samardzija, J. Pastalan, M. MacDonald, S. Walker, and R. Valenzuela, "Compressed transport of baseband signals in radio access networks," *IEEE Trans. Wireless Commun.*, vol. 11, no. 9, pp. 3216–3225, Sep. 2012.
- [20] D. Peng-ren and Z. Can, "Compressed transport of baseband signals in cloud radio access networks," in *Proc. 9th Int. Conf. Commun. Netw. China*, 2014, pp. 484–489.

- [21] Y. Ren, Y. Wang, G. Xu, and Q. Huang, "A compression method for LTE-A signals transported in radio access networks," in *Proc. 21st Int. Conf. Telecommun.*, Lisbon, Portugal, May 2014, pp. 293–297.
- [22] Z. He, C. Hu, T. Peng, and C. Ma, "A compression scheme for LTE baseband signal in C-RAN," in *Proc. 9th Int. Conf. Commun. Netw. China*, Maoming, China, Aug. 2014, pp. 202–207.
- [23] H. Si, B. L. Ng, M. S. Rahman, and J. Zhang, "A novel and efficient vector quantization based CPRI compression algorithm," *IEEE Trans. Veh. Technol.*, vol. 66, no. 8, pp. 7061–7071, Aug. 2017.
- [24] 3GPP TS 36.211, "Evolved universal terrestrial radio access (EUTRA); Physical channels and modulation," Sophia Antipolis Cedex, France, 2010.
- [25] R. M. Gray and D. L. Neuhoff, "Quantization," *IEEE Trans. Inf. Theory*, vol. 44, no. 6, pp. 2325–2383, Oct. 1998.
- [26] S. P. Lloyd, "Least squares quantization in PCM," IEEE Trans. Inf. Theory, vol. IT-28, no. 2, pp. 129–137, Mar. 1982.
- [27] K. J. Kim, J. Yue, R. Iltis, and J. Gibson, "A QRD-M/Kalman filter-based detection and channel estimation algorithm for MIMO-OFDM systems," *IEEE Trans. Wireless Commun.*, vol. 4, no. 2, pp. 710–721, Mar. 2005.
- [28] O. Dizdar and A. O. Yilmaz, "Blind channel estimation based on the Lloyd-Max algorithm in narrowband fading channels and partial-band jamming," IEEE Trans. Commun., vol. 60, no. 7, pp. 1986–1995, Jul. 2012.
- [29] J.-C. Lin, H.-K. Chang, M.-L. Ku, and H. V. Poor, "Impact of imperfect source-to-relay CSI in amplify-and-forward relay networks," *IEEE Trans. Veh. Technol.*, vol. 66, no. 6, pp. 5056–5069, Jun. 2017.
- [30] M. M. Vasconcelos and N. C. Martins, "Optimal estimation over the collision channel," *IEEE Trans. Autom. Control*, vol. 62, no. 1, pp. 321–336, Jan. 2017.
- [31] L. Liu, Y. Li, Y. Su, and Y. Sun, "Quantize-and-forward strategy for interleave-division multiple-access relay channel," *IEEE Trans. Veh. Tech*nol., vol. 65, no. 3, pp. 1808–1814, Mar. 2016.
- [32] M. I. Noah, "Optimal Lloyd-Max quantization of LPC speech parameters," in Proc. Int. Conf. Acoust., Speech, Signal Process., 1984, pp. 19–21.
- [33] C. E. Shannon, "A mathematical theory of communication," *Bell Syst. Tech. J.*, vol. 27, no. 3, pp. 379–423, Jul. 1948.
- [34] D. A. Huffman, "A method for the construction of minimum redundancy codes," *Proc. Inst. Radio Eng.*, vol. 40, pp. 1098–1101, Sep. 1952.
- [35] T. M. Cover and J. A. Thomas, *Elements of Information Theory*. Hoboken, NJ, USA: Wiley, 2006.
- [36] "Study on enhancement of 3GPP support for 5G V2X services (v15.0.0, release 15)," 3GPP, Sophia Antipolis Cedex, France, Tech. Rep. 22.886, Mar. 2017.



Yuhan Su received the B.S. degree from Huaqiao University, Xiamen, China, in 2015. He is currently working toward the Ph.D. degree in communication and information system with Xiamen University Xiamen, China. His research interests include wireless communications, congestion control, radio resource management and network coding.



Xiaozhen Lu received the B.S. degree in communication engineering from the Nanjing University of Posts and Telecommunications, Nanjing, China, in 2017. She is currently working toward the Ph.D. degree with the Department of Communication Engineering, Xiamen University, Xiamen, China. Her research interests include network security and wireless communications.



Lianfen Huang received the B.S. degree in radio physics and the Ph.D. degree in communication engineering from Xiamen University, Xiamen, China, in 1984 and 2008, respectively. She was a Visiting Scholar with Tsinghua University, Beijing, China, in 1997, and with The Chinese University of Hong Kong, Hong Kong, in 2012. She is currently a Professor of communication engineering with Xiamen University. Her research interests include wireless communication, wireless network, and signal process.



Xiaojiang Du (SM'09) received the B.S. and M.S. degrees in electrical engineering from Tsinghua University, Beijing, China, in 1996 and 1998, respectively, and the M.S. and Ph.D. degrees in electrical engineering from the University of Maryland, College Park, MD, USA, in 2002 and 2003, respectively. He is currently a Professor with the Department of Computer and Information Sciences, Temple University, Philadelphia, PA, USA. His research interests include security, wireless networks, and systems. He has authored more than 350 journals and conference

papers in these areas, as well as a book published by Springer. He was the recipient of more than U.S. 5 million research grants from the U.S. National Science Foundation, the Army Research Office, Air Force, NASA, the State of Pennsylvania, and Amazon. He is a Life Member of the ACM. He was the recipient of the Best Paper Award at the IEEE GLOBECOM 2014 and the Best Poster Runner-Up Award at the ACM MobiHoc 2014. He was the Lead Chair of the Communication and Information Security Symposium of the IEEE International Communication Conference 2015 and a Co-Chair of the Mobile and Wireless Networks Track of the IEEE Wireless Communications and Networking Conference 2015.



Mohsen Guizani (S'85–M'89–SM'99–F'09) received the B.S. (Hons.) and M.S. degrees in electrical engineering and the M.S. and Ph.D. degrees in computer engineering from Syracuse University, Syracuse, NY, USA, in 1984, 1986, 1987, and 1990, respectively. He was an Associate Vice President of graduate studies with Qatar University, the Chair of the Computer Science Department, Western Michigan University, and the Chair of the Computer Science Department, University of West Florida. He was also in academic positions with the University of

Missouri-Kansas City, University of Colorado-Boulder, Syracuse University, and Kuwait University. He is currently a Professor and the ECE Department Chair with the University of Idaho, Moscow, ID, USA. He is the Author of nine books and more than 500 publications in refereed journals and conferences. His research interests include wireless communications and mobile computing, computer networks, mobile cloud computing, security, and smart grids. He is a Senior Member of the ACM. He was the recipient of the Wireless Technical Committee's Recognition Award in 2017. He was also the recipient of the Teaching Award multiple times from different institutions, as well as the Best Research Award from three institutions. He was the Chair of the IEEE Communications Society Wireless Technical Committee and the TAOS Technical Committee. He was as a member, the Chair, and the General Chair of a number of international conferences. He was the IEEE Computer Society Distinguished Speaker from 2003 to 2005. He is currently on the editorial boards of several international technical journals and the Founder and the Editor-in-Chief of the Journal of Wireless Communications and Mobile Computing (Wiley). He guest edited a number of special issues in IEEE journals and magazines.